UNSUPERVISED 3D SEGMENTATION OF HIPPOCAMPUS IN BRAIN MR IMAGES

Sandeep S. Kaushik and Jayanthi Sivaswamy
Center for Visual Information Technology, IIIT-Hyderabad, Hyderabad, India

Keywords: Hippocampus, MRI segmentation, Water flow, Deep brain structure, Surface evolution, Region growing, 3D segmentation, Hippocampal volumetry.

Abstract: The most widely followed procedure for diagnosis and prognosis of dementia is structural neuroimaging of hippocampus by means of MR. Hippocampus segmentation is of wide interest as it enables quantitative assessment of the structure. In this paper, we propose an algorithm for hippocampus segmentation that is unsupervised and image driven. It is based on a hybrid approach which combines a coarse segmentation and surface evolution. A coarse solution is derived using region growing which is further refined using a modified version of the physics based water flow model (Liu and Nixon, 2007). The proposed method has been tested on a publicly available dataset. The performance of this method is assessed using Dice coefficient against the ground truth provided for 25 volume images. It is consistent across volumes and the average Dice values are comparable to a multi-atlas based method reported on a subset of the same dataset.

1 INTRODUCTION

Dementia is a clinical syndrome that affects memory and cognitive ability of a person. It is known to be caused due to traumatic brain injury, neurodegenerative diseases, bacterial infections, prolonged epileptic seizures, and so on. Some common types of dementia are mild cognitive impairment (MCI) or incipient dementia, Alzheimer disease (AD) or dementia of the Alzheimer type (DAT), dementia with Lewy bodies (DLB) and fronto-temporal dementia (FTD). Dementia is usually diagnosed based on clinical observations, presence of characteristic neurological and neuropsychological features. Onset of dementia is difficult to diagnose with these methods. Therefore, along with clinical diagnosis, structural neuroimaging is used to enable early diagnosis so that it can be treated at the onset. Apart from diagnosis, structural neuroimaging helps to distinguish between different types of dementia, to differentiate between normal aging and dementia and in differential diagnosis. Some of the methods to assess change in brain volume by means of structural neuroimaging are volumetry, voxel based morphometry (VBM), cortical pattern matching and brain boundary shift integral measurements. Hippocampus is the structure responsible for long term memory in the brain and its atrophy is an early and specific marker of dementia. The severity of hippocampal atrophy is directly related to progress of the underlying disease and hence reflects the extent of cognitive impairment. Although atrophy rates have been observed to be larger in entorhinal cortex than in hippocampus, difficulty in unambiguously defining this structure makes its measurement highly variable. Thus, hippocampus is the region of interest in differential diagnosis of AD and mild cognitive impairment (MCI).

Manual labelling by experts is considered as gold standard of hippocampal segmentation. But this is laborious, time consuming, prone to inconsistency and inter-expert labelling variability. Advanced image analysis techniques have been used to minimise these problems by developing semi-automatic hippocampal segmentation methods or further, by obtaining reliable initialisation, fully automatic segmentation methods. From medical imaging viewpoint, research in segmentation of deep brain structures in general and hippocampus in particular is motivated by various factors like i) development of computer aided diagnosis solution by methods. The attraction here is the potential for high precision and consistency over manual segmentation which in turn offers reliable volumetry (Bernasconi et al., 2003); ii) study of the characteristic pattern of a particular disease or normal aging (Chupin et al., 2008); iii) development of generalised segmentation algorithm applicable to

S. Kaushik S. and Sivaswamy J..
UNSUPERVISED 3D SEGMENTATION OF HIPPOCAMPUS IN BRAIN MR IMAGES.
DOI: 10.5220/0003145401820187
In *Proceedings of the International Conference on Bio-inspired Systems and Signal Processing* (BIOSIGNALS-2011), pages 182-187
ISBN: 978-989-8425-35-5

various structures (Morra et al., 2008); iv) acceleration of drug trials and population study of diseases. In general, the hippocampus, with weak edges and inhomogeneity, acts as a good test case for a neurosegmentation algorithm in both 2D and 3D (Morra et al., 2010). Given the focus of this paper on hippocampus segmentation, next section reviews the existing methods for the same in some detail.

1.1 Related Work

The existing methods can be classified broadly based on the approach taken to include the domain knowledge as follows: i) atlas and cohort atlas based, ii) pattern classification and machine learning methods based and iii) deformable models or template based.

Segmentation via registration to a brain atlas is class of methods followed in (Akhondi-Asl et al., 2010; Ltjnen et al., 2010). In these methods, a neuroanatomic atlas is registered, i.e., spatially aligned with the given subject image to delineate the boundary of the region of interest. The registration is carried out after geometric transformation to correct alignment and enhancement to correct intensity variations. Atlas-based approaches have the advantage that advances in registration techniques can be exploited. Thus, most of the available standard registration algorithms and packages can be used for segmentation. Standard atlases available are Harvard whole brain atlas and MNI-Talairach atlas. They contain the labelled structures of the whole brain and hence can be used to segment any structure without prior knowledge about the structure. However, if the subject image varies largely from the atlas in terms of age of the subject or physical dimensions of the voxels, segmentation performance suffers. To overcome this issue, a cohort atlas is built. In cohort atlas, experts manually segment the structure of interest on one or more subject images selected from a set of reference images. Each or combination of these labelled data (image) can be used as an atlas. The disadvantage of using cohort atlas is the requirement of an expert and one or more labelled data. Both of these methods have the common issue of inability to handle variation in data over larger sets. Hence, atlases are more suitable for initialisation than for complete segmentation.

An alternative way to use domain knowledge is with pattern classification and machine learning techniques. Statistical and anatomical prior knowledge are learnt and used to localise and segment hippocampus. Appearance based features are used to build a context model in (Morra et al., 2010), while segmentation is posed as an expectation maximisation problem in (Sabuncu et al., 2009). Prior information from an atlas and segmentation via likelihood has been adopted in (Akselrod-Ballin et al., 2007). Most of the techniques depend upon the shape of hippocampus varying within a given margin. Furthermore, since these techniques are largely supervised, the choice of features and modelling of the problem is critical.

Template and deformable models help use domain knowledge in a more flexible way. These methods are derived by using prior anatomical knowledge. The structure to be segmented is modelled and parameterised using shape knowledge and then deformed to segment the structure. Minimising an energy function via iterated conditional modes (ICM), initialised by prior information from probabilistic atlas is described in (Chupin et al., 2008). Although these methods have been observed to perform well, their design and implementation are very complex. Shape encoding for segmentation has to consider all possible variations of shape of the structure. This requires a large amount of supervision to train the model. In some of these methods, anatomical information derived depends on landmark detection.

In general, while prior knowledge about brain structures can aid the segmentation problem, there are some costs involved in acquiring this knowledge and obtaining a good and consistent segmentation performance: i) adequate amount of labelled data for training, ii) age, race and disease-specific matched information. An alternative is to use an unsupervised, hybrid approach. A combination of region growing and deformable model or curve evolution is one such option. Region growing is a relatively fast algorithm which can extract all parts of the region like curves and narrow parts. In most of the imaging modalities like optical, CT and MRI, with appropriate features used for determining homogeneity criteria, region growing proves to be one of the simplest methods of segmentation. However, this alone does not result in an exact boundary as region growing is vulnerable especially to weak edges and non-homogeneous regions. The second curve evolution stage is employed to address this problem. The resulting surface is taken as input to surface evolution. This is more accurate than the conventional simple geometric surface initialisation and much faster than manual surface initialisation. Surface evolution merely needs to adjust the surface to exact boundaries which results in quick convergence. An image foresting transform (IFT) for coarse segmentation together with an active surface solution has been proposed for liver segmentation in CT (Pohle et al., 2003).

In this paper, a non-parametric, hybrid method is proposed for hippocampus segmentation which utilises only local image information. The method

follows the coarse segmentation and surface evolution framework with the key differences being: the surface is not parameterised and is evolved using a physics based water flow model (Liu and Nixon, 2007). The water flow model has been applied to 2D image segmentation of synthetic images. It has been demonstrated (but not rigorously assessed) on some 2D real cases such as grey-white matter interface, femur from MRI, carotid artery in MR angiogram and retinal vessels; and 3D lateral ventricles. Most of these structures are homogeneous with well defined boundaries. In this paper, it is demonstrated how the water flow model can be adapted to a relatively inhomogeneous, partially weak edged hippocampus. It is demonstrated that, in spite of its simplicity, our hybrid algorithm yields results comparable to a recently reported method. The following section describes this method in detail.

2 HYBRID SEGMENTATION

The water flow model directs the progress of a water front based on local image properties derived from region and edge based forces. In this paper, this model is chosen because of the following features: i) it is a physics based model which does not depend on image topology and ii) it makes use of both gradient forces and region based forces which is attractive given the weak edged boundary of the hippocampus.

Since the water flow algorithm acts on a water front, one of the simplest methods to obtain a front is by coarse segmentation via region growing. The coarse segmentation stage works on intensity features which are sensitive to intensity variation due to a bias field that can be present. In order to address this problem, the image volume is pre-processed for bias field correction. A modified fuzzy C-means algorithm proposed in (Ahmed et al., 2002) is used for this purpose. Here, the intensity inhomogeneity is estimated using fuzzy logic and used to correct the slowly varying shading artefact over the image.

2.1 Coarse Segmentation

This stage begins with few seeds initialised by the user. The protocol of choosing multiple seeds, instead of one, is used so that longitudinal extremes of hippocampus can be approximated and an initial modelling of intensity variation can be obtained. In the process of region growing, these seeds are used to check for homogeneity in their immediate neighbourhood and decide whether or not to include those voxels into the region. The parameters used in homogeneity verification are: deviation of a candidate's voxel value from the mean voxel value of the region and the gradient magnitude at the candidate voxel's location.

2.2 Fine Segmentation

The original water flow algorithm (Liu and Nixon, 2007) computes a resultant force on a voxel due to its neighbouring voxels and decides the flow action. Three types of image forces, namely, field, potential and statistical forces aid or oppose the flow, based on their direction with respect to the resultant field force.

The Field force experienced by a voxel at position $\mathbf{r}_i$ due to its neighbourhood W is given by the force field transformation (Hurley et al., 2005) as

$$\mathbf{F}_f(\mathbf{r}_i) = \sum_{j \in W, j \neq i} L(r_j) \frac{(\mathbf{r}_j - \mathbf{r}_i)}{|\mathbf{r}_j - \mathbf{r}_i|^3} \quad (1)$$

The elements of L matrix are set to -1 when a voxel is filled with water (it is inside the region) and set to the gradient magnitude (edge strength) otherwise. This results in a force which is always directed away from the region. In a cross-sectional area A (set to unity), the flow velocity gained by a voxel is

$$\mathbf{v} = \frac{\mathbf{F}_f(\mathbf{r}_i)}{AR} \quad (2)$$

where R is the flow resistance given by

$$R = e^{k\mathbf{E}(\mathbf{r}_i)} \quad (3)$$

where $\mathbf{E}(\mathbf{r}_i)$ is the edge strength (magnitude of the gradient) at location $\mathbf{r}_i$ and k is the resistance controlling factor. Higher values of k leads to higher sensitivity to edges.

In addition to the static field force $\mathbf{F}_f(\mathbf{r}_i)$, image forces such as potential force, statistical force contribute to the element flow. The potential force is calculated based on the gradient of the edge map $\mathbf{E}$. This force is largely concentrated around the edges in the image and hence acts as a barrier to the water flow. In the known direction of flow i, given a target position $\mathbf{r}_t$, the potential force experienced by the flowing element is given by

$$F_{p,i} = \nabla \mathbf{E}(\mathbf{r}_t) \quad (4)$$

Water flow model also uses a region based statistical force based on the Mumford-Shah functional. It reflects the change in internal and external intensities of a closed region and its surroundings. When the target voxel intensity deviates largely from the equilibrium, this force turns negative and hence checks the flow.

Statistical force due to a target voxel at position $\mathbf{r}_t$ is given by

$$F_{s,i} = \frac{n_{ext}}{n_{ext}+1}(I(\mathbf{r}_t)-\mu_{ext})^2 - \frac{n_{int}}{n_{int}+1}(I(\mathbf{r}_t)-\mu_{int})^2 \quad (5)$$

where $I(\mathbf{r}_t)$ is the intensity value at voxel position $\mathbf{r}_t$, n is the number of voxels and μ is the mean of intensity of the internal and external regions denoted by the subscripts *int* and *ext* respectively. To maintain a balance in the simultaneous contribution of these forces in the element flow, they are added by a convex equation as

$$F_i = \alpha F_{p,i} + (1-\alpha)F_{s,i} \quad (6)$$

In the original water flow algorithm, the flow of an individual waterfront voxel is not constrained explicitly by other voxels in the front. However, its movement should be dependent on the mobility of its surrounding voxels on the surface and the tension between these voxels. Hence, a new *tensile* force component is introduced which has the effect of opposing the flow. This force controls the stretching of the surface and ensures a continuous surface without holes. The tensile force experienced by a voxel at $\mathbf{r}_i$ is calculated using the umbrella operator approximation of Laplacian given by (McInerney and Terzopoulos, 1999) as

$$F_{t,i} = \frac{1}{n}\sum_{j\in N}(\mathbf{r}_j - \mathbf{r}_i) \quad (7)$$

where $\mathbf{r}_j$is the position of the j^{th} surface voxel within N neighbourhood of $\mathbf{r}_i$ and n is the total number of voxels in that neighbourhood.

The work done by a voxel under the influence of all the forces combined is given by

$$J = \frac{m|\mathbf{v}_i|^2}{2} + (F_i - \eta F_{t,i})S \quad (8)$$

where m is mass of the element analogous to intensity of the voxel and S is the preset displacement. If work done is positive, the element moves in the direction of the resultant force for a predetermined (fixed) distance. η controls the influence of the tensile force experienced by the surface.

3 EXPERIMENTS AND RESULTS

User initialised seed points (minimum 1 per slice) are collected along the length of hippocampus in the coronal view of a brain MR volume image. Based on the extreme points, with reasonable margin on all sides, a sub volume is extracted for faster processing. To make sure the surface evolves properly to match both these shapes, two sets of parameters of surface evolution - α, η and S are used, one to suit head region and one to suit the body-tail region.

The proposed method is tested on a publicly available brain MR dataset (Jafari-Khouzani, 2010). It consists of 25 volumes of training data with associated ground truth and 25 volumes of testing data without any ground truth. The first (training) set has been chosen as the test data. This set consists of 15 volumes of T1-weighted MR image data of each slice 256x256 pixels with voxel size 0.781x0.781x2.00mm^3 and 10 volumes of T1-weighted MR image data of each slice 512x512 pixels with voxel size 0.39x0.39x2.00mm^3. Assessment is done by computing the Dice coefficient.

Table 1: Comparison of performance with and without tensile force.

	Dice's coefficient		
Water flow model	Min.	Max.	Avg.
With tensile force	0.63	0.72	0.68 ± 0.03
Without tensile force	0.49	0.68	0.62 ± 0.06

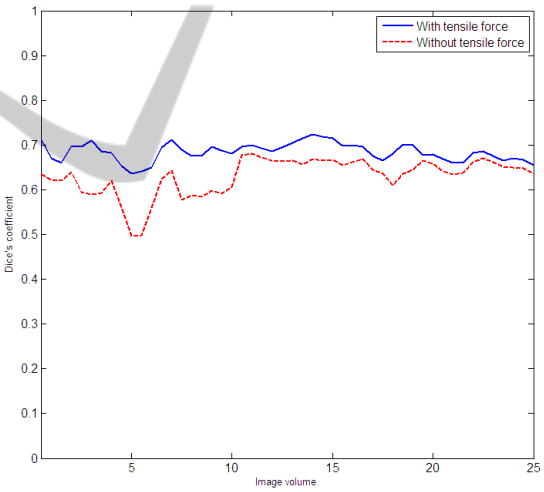

Figure 1: Comparison of performance with and without tensile force.

Since a new tensile component was introduced in the water flow algorithm, in order to assess its effectiveness, the Dice coefficient was calculated for the proposed method with and without this component. Table 1 shows the maximum, minimum and the average Dice coefficient for 50 hippocampi in the test set. It can be observed from the table that the tensile force component plays a positive role in segmentation and contributes to 6% improvement, on average, in the Dice coefficient. The dataset (Jafari-Khouzani, 2010) has also been used for assessment of a multi-atlas (derived from 10 subjects) based method proposed in (Akhondi-Asl et al., 2010) which reports the

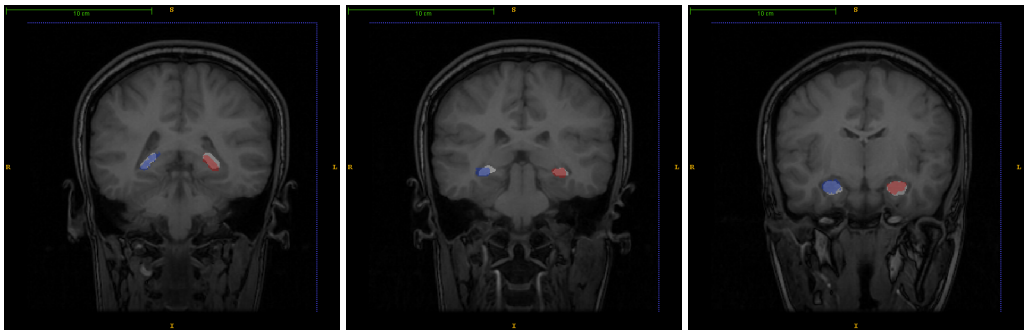

(a) Tail. (b) Body. (c) Head.

Figure 2: Overlay of algorithm output with manual label. Red and Blue translucent regions correspond to algorithm output and white opaque regions correspond to manual label.

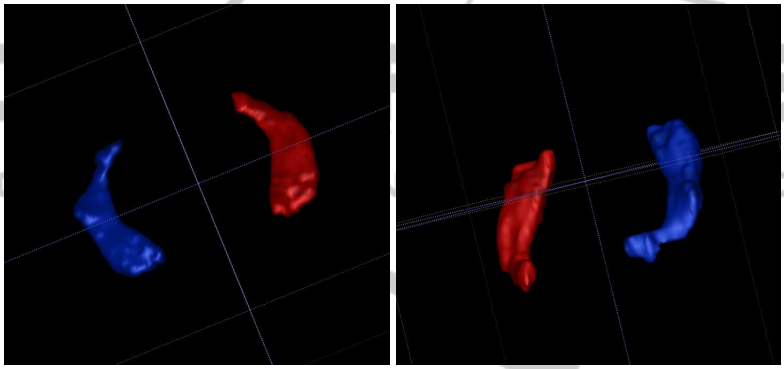

(a) 3D view from hippocampus head. (b) 3D view from hippocampus tail.

Figure 3: 3D surface view of the algorithm output.

average Dice coefficient for the testing part of the dataset as (0.72 ± 0.09). This is comparable to that (0.68 ± 0.03) obtained on the training subset by the proposed method despite the major difference in the approaches behind the two methods: multiple atlases based versus unsupervised method.

Figure 1 provides a graphical comparison of the Dice coefficient for every volume. The trend of the two plots is approximately similar. This trend is consistent with the fact that, by design, the tensile force plays only a moderating role as per (8). In general, it was observed that the segmentation performance drops when, even in absence of atrophy, size of hippocampus was very small. In such cases, the cortical walls surrounding the hippocampus and the neighbouring amygdala make the true boundary difficult to detect resulting in an over-segmentation.

Figure 2 shows some sample extracted hippocampi overlaid over the ground truth. The translucent regions of red and blue denote segmented left and right hippocampus respectively by the proposed method. The opaque white region under these corresponds to manual label which is used as the ground truth. Figure 3 shows the 3D surface view of segmented hippocampi as seen from head of the hippocampus in Figure 3(a) and as seen from its tail in Figure 3(b).

4 CONCLUSIONS

In this paper, a new method for segmentation of hippocampus in MR volume images is proposed. The advantage of this method is that it does not require an atlas or template and is free of parameterisation and supervision. In spite of its simplicity, this method's performance is comparable to existing methods. The tight variance in the Dice coefficient is particularly encouraging. These results demonstrate that the framework of hybrid segmentation can successfully tap advantages of each of the two stages.

The improvement in segmentation performance with the addition of the proposed tensile component to the water flow model indicates that the surface evolution is constrained yet yields more accurate sur-

faces. A shortcoming of the proposed methods is that since the water flow model always evolves from inside the region to outside, the coarse segmentation output has to be within the target boundary of the hippocampus. This limitation can be addressed by designing techniques which permit a two-sided evolution of the water front.

Overall, it can be concluded that the obtained results show promise and pave way for applying of the water flow model for segmenting other (partially) weak-edge structures as well. Future work will be targeted at complete automation of this method by reliable automatic initialisation of seed points or replacing the region growing with any other method for coarse segmentation.

ACKNOWLEDGEMENTS

The authors would like to thank Dr. D.Ravi Varma, DM, KIMS hospital, Hyderabad for his input towards anatomical structure of hippocampus and qualitative analysis of results.

REFERENCES

Ahmed, M., Yamany, S., Mohamed, N., Farag, A., and Moriarty, T. (2002). A modified fuzzy c-means algorithm for bias field estimation and segmentation of mri data. *Medical Imaging, IEEE Transactions on*, 21(3):193 – 199.

Akhondi-Asl, A., Jafari-Khouzani, K., Elisevich, K., and Soltanian-Zadeh, H. (2010). Hippocampal volumetry for lateralization of temporal lobe epilepsy: Automated versus manual methods. *NeuroImage*, In Press, Corrected Proof:–.

Akselrod-Ballin, A., Galun, M., Gomori, J. M., Brandt, A., and Basri1, R. (2007). Prior knowledge driven multiscale segmentation of brain mri. *MICCAI 2007*, 4792/2007:118–126.

Bernasconi, N., Bernasconi, A., Caramanos, Z., Antel, S. B., Andermann, F., and Arnold, D. L. (2003). Mesial temporal damage in temporal lobe epilepsy: a volumetric MRI study of the hippocampus, amygdala and parahippocampal region. *Brain*, 126(2):462–469.

Chupin, M., Cuingnet, R., Lemieux, L., Lehericy, S., Benali, H., Garnero, L., and Colliot, O. (2008). Fully automatic hippocampus segmentation discriminates between alzheimer's disease and normal aging - data from the adni database. In *MICCAI Workshop on CAPH*.

Hurley, D. J., Nixon, M. S., and Carter, J. N. (2005). Force field feature extraction for ear biometrics. *Computer Vision and Image Understanding*, 98(3):491 – 512.

Jafari-Khouzani, K. (2010). Mri data set for hippocampus segmentation by department of diagnostic radiology at henry ford hospital. http://www.radiologyresearch.org/HippocampusSegmentationDatabase/.

Liu, X. U. and Nixon, M. S. (2007). Image and volume segmentation by water flow. In *ISVC'07: Proceedings of the 3rd international conference on Advances in visual computing*, pages 62–74, Berlin, Heidelberg. Springer-Verlag.

Ltjnen, J. M., Wolz, R., Koikkalainen, J. R., Thurfjell, L., Waldemar, G., Soininen, H., and Rueckert, D. (2010). Fast and robust multi-atlas segmentation of brain magnetic resonance images. *NeuroImage*, 49(3):2352 – 2365.

McInerney, T. and Terzopoulos, D. (1999). Topology adaptive deformable surfaces for medical image volume segmentation. *Medical Imaging, IEEE Transactions on*, 18(10):840 –850.

Morra, J., Tu, Z., Apostolova, L., Green, A., Toga, A., and Thompson, P. (2008). Automatic subcortical segmentation using a novel contextual model. *MICCAI*.

Morra, J., Tu, Z., Apostolova, L., Green, A., Toga, A., and Thompson, P. (2010). Comparison of adaboost and support vector machines for detecting alzheimer's disease through automated hippocampal segmentation. *Medical Imaging, IEEE Transactions on*, 29(1):30 – 43.

Pohle, R., Behlau, T., and Toennies, K. D. (2003). Segmentation of 3d medical image data sets with a combination of region-based initial segmentation and active surfaces. *Medical Imaging 2003: Image Processing*, 5032:1225–1232.

Sabuncu, M. R., Yeo, B. T., Leemput, K., Fischl, B., and Golland, P. (2009). Supervised nonparametric image parcellation. In *MICCAI 2009*, pages 1075–1083, Berlin, Heidelberg. Springer-Verlag.